ELECTRON DIFFRACTION PATTERNS ANALYSIS OF PRECIPITATES IN LD_{10} ALLOY①

Jin, Tounan Yin, Zhimin
Department of Materials Science and Engineering,
Central South University of Technology, Changsha 410083

ABSTRACT By means of the available crystal parameters of precipitates and the orientation relationships between the precipitates and the matrix in aluminium alloys, the diffraction patterns of all possible precipitates have been simulated, which agrees with experimental observations in LD_{10} alloy. The method used was to transform the reciprocal lattice vectors $\boldsymbol{g}_p$ of the precipitate phases into unit normal vector on the matrix lattice, and to check up whether those $\boldsymbol{g}_p$ satisfy the Bragg condition and then to determine the locations of diffraction spots on the matrix diffraction pattern. The method is applicable to any system where the orientation relationships and lattice parameters of matrix and precipitate phase are known.

Key words precipitate simulated diffraction pattern transformation matrix

1 INTRODUCTION

The commercial LD_{10} alloy is a kind of deformation aluminium alloy which is mainly used in making large-size forgings. As generally known, during aging of LD_{10} alloy there are two kinds of primary precipitation sequences, i.e. $Mg_2Si(\beta)$ and $CuAl_2(\theta)$ precipitates and minority $Al_2CuMg(S)$ sequence precipitates[1]. Because of the similarity of morphology, precipitation processing and orientation relationship of these precipitates[1,2], there is apparent confusion when the phase identification is made, especially by using SADP. In this paper, crystal direction index transformation matrix between the precipitates and the matrix has been set up in order to find out the reflection planes of the precipitates satisfying the Bragg condition, and an unambiguous interpretation of the SADP has been mode.

2 EXPERIMENTAL

The tested material was cut from the hot rolled plate of the LD_{10} alloy supplied by the Northeast Light Metal Working Plant. The nominal composition (%) of this alloy is Al-(3.9～4.8)Cu-(0.4～0.8)Mg-(0.6～1.2)Si-(0.4～1.0)Mn-0.12Ti. Some pieces were cut and solution treated at 503 ℃ for 50 min, then quenched into 25 ℃ water. Aging treatment was carried out in an air furnace at 236 ℃ for 24 h.

The thin foils were prepared using a jet electro-polishing technique in a 30% nitric acid-methanol bath at − 25 ℃. The electropolished discs were examined in a H-800 electron microscope at 175 kV.

3 THEORETICAL SIMULATED DIFFRACTION PATTERNS OF PRECIPITATES

3.1 *Orientation Relationships between Precipitates and Matrix*

During aging, before the equilibrium β (Mg_2Si), θ($CuAl_2$) and S(Al_2CuMg) formed, some corresponding transition phases marked

① Supported by the special fund of China National Education Committee; received Jun. 15, 1995

Table 1 Crystal parameters of the primary precipitates existing in LD_{10} alloy

precipitate	crystal structure	lattice parameter / Å	orientation relationship
β'	hexagonal	$a=7.05$, $c=4.05$	$\{001\}_{\beta'} // \{100\}_\alpha$, $\langle 010\rangle_{\beta'} // \langle 110\rangle_\alpha$
β	cubic	a=6.42	$\{001\}_\beta // \{001\}_\alpha$, $\langle 010\rangle_\beta // \langle 110\rangle_\alpha$
θ'	tetragonal	$a=b=4.04$, $c=5.80$	$\{001\}_{\theta'} // \{001\}_\alpha$, $\langle 010\rangle_{\theta'} // \langle 110\rangle_\alpha$
θ	tetragonal	$a=b=6.07$, $c=4.87$	$\{001\}_\theta // \{001\}_\alpha$, $\langle 010\rangle_\theta // \langle 120\rangle_\alpha$
S	orthorhombic	$a=4.00$, $b=9.23$, $c=7.14$	$\{001\}_S // \{001\}_\alpha$, $\langle 010\rangle_S // \langle 120\rangle_\alpha$

as β', θ' and S' phases would precipitate. Among them the S' phase has the same crystal structure as the S phase only with slight difference in lattice parameters[5]. Therefore, the crystal parameters are not distinguished between the S' and S phase. The crystal parameters of the primary percipitates existing in LD_{10} alloy are summed up in Table 1[2, 3].

In order to set up the crystal direction index transformation matrix between precipitates and matrix, the orientation relationship between the precipitates and the matrix has to be determined, which can be obtained through analyzing the data presented in Table 1. The orientation relationships between β', β, S phases and the matrix are listed in Table 2. The subscript of the precipitate symbol stands for the type of the orientation relationship, which is called variant. For example, S_9 stands for 9th variant of the S phase. The θ' phase has six variants, and their expressions of orientation relationship indexes are the same as that of β phase. The θ phase has twelve variants, and their experessions of orientation relationship indexes are the same as that of S phase.

3.2 *Direction Index Transformation Matrix between Precipitates and Matrix*[4]

Suppose the orientation relationship between a precipitate (p) and matrix (α) are $[100]_p // [m_1n_1p_1]_\alpha$, $[010]_p // [m_2n_2p_2]_\alpha$ and $[001]_p // [m_3n_3p_3]_\alpha$. $[m_in_ip_i]_\alpha$ is a normalized unit vector, the crystal direction of the matrix (X_α) and the precipitate (X_p) can be connected with a transformation matrix (M). That is

$$X_p = MX_\alpha,\ M = \begin{bmatrix} m_1 & n_1 & p_1 \\ m_2 & n_2 & p_2 \\ m_3 & n_3 & p_3 \end{bmatrix}$$

then

$$X_\alpha = M^{-1}X_p \tag{1}$$

$$M^{-1} = M' = \begin{bmatrix} m_1 & m_2 & m_3 \\ n_1 & n_2 & n_3 \\ p_1 & p_2 & p_3 \end{bmatrix} \tag{2}$$

Thus, through equations (1), (2) and Table 2, any crystal direction in the precipitate can be represented using a certain crystal direction in matrix.

Table 2 The orientation relationship between precipitate β, β', S and the matrix

precipitate	orientation relationship
β'_1	$[100]_{\beta'} // [110]_\alpha$, $[001]_{\beta'} // [001]_\alpha$
β'_2	$[010]_{\beta'} // [110]_\alpha$, $[001]_{\beta'} // [001]_\alpha$
β_1	$[100]_\beta // [100]_\alpha$, $[010]_\beta // [011]_\alpha$, $[001]_\beta // [0\bar{1}1]_\alpha$
β_2	$[100]_\beta // [100]_\alpha$, $[010]_\beta // [0\bar{1}1]_\alpha$, $[001]_\beta // [0\bar{1}\bar{1}]_\alpha$
β_3	$[100]_\beta // [010]_\alpha$, $[010]_\beta // [101]_\alpha$, $[001]_\beta // [\bar{1}0\bar{1}]_\alpha$
β_4	$[100]_\beta // [010]_\alpha$, $[010]_\beta // [\bar{1}01]_\alpha$, $[001]_\beta // [\bar{1}0\bar{1}]_\alpha$
β_5	$[100]_\beta // [001]_\alpha$, $[010]_\beta // [110]_\alpha$, $[001]_\beta // [1\bar{1}0]_\alpha$
β_6	$[100]_\beta // [001]_\alpha$, $[010]_\beta // [1\bar{1}0]_\alpha$, $[001]_\beta // [\bar{1}\bar{1}0]_\alpha$
S_1	$[100]_S // [100]_\alpha$, $[010]_S // [021]_\alpha$, $[001]_S // [0\bar{1}2]_\alpha$
S_2	$[100]_S // [100]_\alpha$, $[010]_S // [012]_\alpha$, $[001]_S // [0\bar{2}1]_\alpha$
S_3	$[100]_S // [100]_\alpha$, $[010]_S // [0\bar{1}2]_\alpha$, $[001]_S // [0\bar{2}\bar{1}]_\alpha$
S_4	$[100]_S // [100]_\alpha$, $[010]_S // [0\bar{2}1]_\alpha$, $[001]_S // [0\bar{1}\bar{2}]_\alpha$
S_5	$[100]_S // [010]_\alpha$, $[010]_S // [201]_\alpha$, $[001]_S // [\bar{1}02]_\alpha$
S_6	$[100]_S // [010]_\alpha$, $[010]_S // [102]_\alpha$, $[001]_S // [\bar{2}01]_\alpha$
S_7	$[100]_S // [010]_\alpha$, $[010]_S // [\bar{1}02]_\alpha$, $[001]_S // [\bar{2}0\bar{1}]_\alpha$
S_8	$[100]_S // [010]_\alpha$, $[010]_S // [\bar{2}01]_\alpha$, $[001]_S // [\bar{1}0\bar{2}]_\alpha$
S_9	$[100]_S // [001]_\alpha$, $[010]_S // [120]_\alpha$, $[001]_S // [2\bar{1}0]_\alpha$
S_{10}	$[100]_S // [001]_\alpha$, $[010]_S // [210]_\alpha$, $[001]_S // [1\bar{2}0]_\alpha$
S_{11}	$[100]_S // [001]_\alpha$, $[010]_S // [2\bar{1}0]_\alpha$, $[001]_S // [\bar{1}\bar{2}0]_\alpha$
S_{12}	$[100]_S // [001]_\alpha$, $[010]_S // [1\bar{2}0]_\alpha$, $[001]_S // [\bar{2}\bar{1}0]_\alpha$

3.3 *Locations of Diffraction Spots of* S *Phase on Matrix* $[001]_\alpha$ *Zone Pattern*

Table 3 The reflection planes satisfying the Bragg condition for variant S_1, S_2, S_3 and S_4

variant	S_1		S_2		S_3		S_4	
plane	$(13\bar{1})_S$	$(1\bar{3}1)_S$	$(11\bar{2})_S$	$(1\bar{1}2)_S$	$(\bar{1}\bar{1}\bar{2})_S$	$(\bar{1}12)_S$	$(\bar{1}\bar{3}\bar{1})_S$	$(\bar{1}31)_S$
g_s direction	$[570]_\alpha$	$[5\bar{7}0]_\alpha$	$[560]_\alpha$	$[5\bar{6}0]_\alpha$	$[\bar{5}60]_\alpha$	$[\bar{5}\bar{6}0]_\alpha$	$[\bar{5}70]_\alpha$	$[\bar{5}\bar{7}0]_\alpha$

Because the content of the precipitates is small, only those stronger reflections of the S phase are expected to form diffraction spots that can be detected. From the PDF data of the S phase, those strong reflection plane indexes are {020}, {002}, {111}, {112}, {131} and {113}. When the incident beam parallels to $[001]_\alpha$, only those planes whose reciprocal vectors $\boldsymbol{g}_s$ nearly perpendicular to $[001]_\alpha$ will be able to satisfy the Bragg condition, and their diffraction spots may be appear at the $[001]_\alpha$ zone pattern. The way to find out these reflection planes is to use the equation (1) and (2) and Table 2 to check up if $\boldsymbol{g}_s$ vectors are perpendicular to $[001]_\alpha$. The calculation sample as follows:

For variant S_1, the transformation matrix is

$$M_{S_1}^{-1} = \begin{bmatrix} 1 & 0 & 0 \\ 0 & \frac{2}{\sqrt{5}} & \frac{-1}{\sqrt{5}} \\ 0 & \frac{1}{\sqrt{5}} & \frac{2}{\sqrt{5}} \end{bmatrix} \qquad (3)$$

For the S phase, the normal vector of the (hkl) plane is parallel to $[h/a, k/b, l/c]_S$. Thus the unit normal vector of $(13\bar{1})_{S_1}$ plane is $X'_{S_1}=[0.5778, 0.7495, \overline{0.3233}]_{S_1}$, then $X'_\alpha=[0.5778, 0.8150, 0.0460]_\alpha$. It is easy to be approved that the reciprocal vector of $(13\bar{1})_{S_1}$ is approximately perpendicular to the $[001]_\alpha$ since X'_α nearly equals $[570]_\alpha$. Among the other strong planes the reciprocal vector of the $(13\bar{1})_{S_1}$ is also nearly perpendicular to $[001]_\alpha$. So for the S_1 variant, only $(13\bar{1})_{S_1}$ and $(1\bar{3}1)_{S_1}$ can satisfy the Bragg condition, and their diffraction spots are located in the directions of $[570]_\alpha$ and $[5\bar{7}0]_\alpha$ respectively and the distances from the origin can be calculated from their lattice spacings. Repeating the process metioned above, the strong reflection planes which satisfy the Bragg condition for variant S_2, S_3 and S_4 and the directions of their reciprocal vectors in the matrix are able to be found out (Table 3). According to the data in Table 3, the locations of diffraction spots of S phase on the matrix $[001]_\alpha$ zone pattern are plotted in Fig. 1(a). On acccount of the symmetry of the crystal, the diffraction spot locations on $[001]_\alpha$ zone pattern for variant S_5, S_6, S_7 and S_8 can be determined by rotating about $[001]_\alpha$ by 90° relative to Fig. 1(a). Considering double diffraction spots of S caused by strong $\{200\}_\alpha$ matrix reflections, the full simulated diffraction pattern should be plotted as Fig. 1 (b). Through the calculation, we can find that the diffraction spots of variant S_9, S_{10}, S_{11} and S_{12} are overlapped with some diffraction spots produced by the former eight variants.

3.4 *Theoretical Simulated Pattern of θ′, θ, β′ and β Phase*

For θ', θ, β' and β phases, the strong reflection plane types satisfying the Bragg condition obtained by calculation are listed in Table 4. Considering the symmetries between the variants, if we know two plane reflection locations for a phase, the others will be obtained by rotation symmetry operation. The simulated results of diffraction patterns for the four precipitates are shown in Fig. 2.

4 RESULTS AND DISCUSSION

A typical example of bright-field TEM image of the specimen aged at 236 ℃ for 24 h is shown in Fig. 3(a), and its SADP is shown in Fig. 3(b). Clearly, it is difficult to identifiy there are how many kinds of precipitates from the complex SADP and the morphologies of

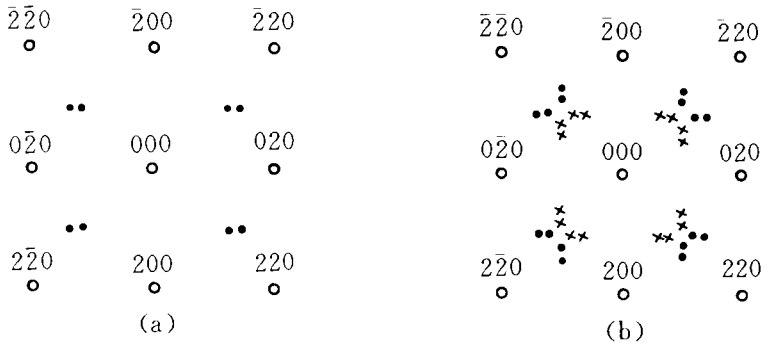

Fig. 1 Theoretical simulated diffraction pattern of *S* phase

(a)—diffraction spots caused by variant S_1, S_2, S_3 and S_4;
(b)—full simulated diffraction pattern
○—matrix $[001]_\alpha$ diffraction; ●—*S* phase diffraction;
×—*S* phase double diffraction caused by $\{200\}_\alpha$ diffraction

Tabele 4 Strong reflection plane types for θ', θ, β' and β phases

phase	θ'		θ		β'		β	
plane type	$(110)_{\theta'}$	$(2\bar{1}1)_{\theta'}$	$(112)_\theta$	$(200)_\theta$	$(010)_{\beta'}$	$(\bar{1}10)_{\beta'}$	$(11\bar{1})_\beta$	$(220)_\beta$
gp direction	$[110]_\alpha$	$[530]_\alpha$	$[380]_\alpha$	$[100]_\alpha$	$[010]_\alpha$	$[\bar{9}50]_\alpha$	$[7100]_\alpha$	$[010]_\alpha$

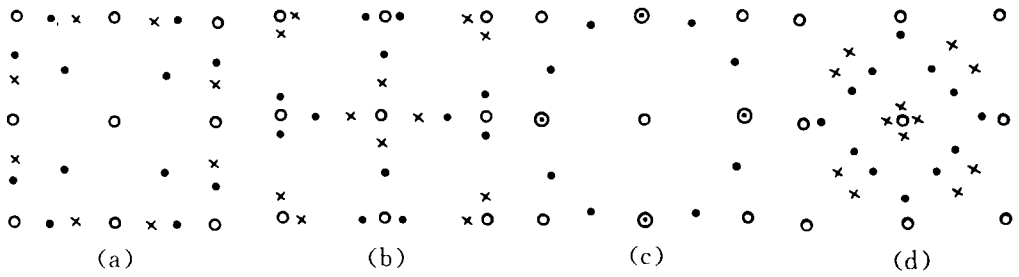

Fig. 2 Theoretical simulated pattern for four precipitates

(a)—θ' phase; (b)—θ phase; (c)—β' phase; (d)—β phase
○—matrix $[001]_\alpha$ reflection; ●—precipitates reflection;
×—precipitates double diffraction caused by $\{200\}_\alpha$ reflection

these precipitates. However, comparing the SADP with the theoretical simulated patterns, we can indicate that the three kinds of precipitates have all occured. On the contrary, it is also confirmed that the results of theoretical calculation is correct. In addition the coincidence of the double diffraction spots on the theoretical pattern with the certain diffraction spots on the practical pattern shows that the double diffractions of the precipitate caused by the strong matrix reflections exist indeed. As generally known, β and θ phases are the primary strengthening phases in LD_{10} alloy and the amount of *S* phase is small[1]. However, in this study from the diffraction strength of *S* phase on the experimental diffraction pattern,

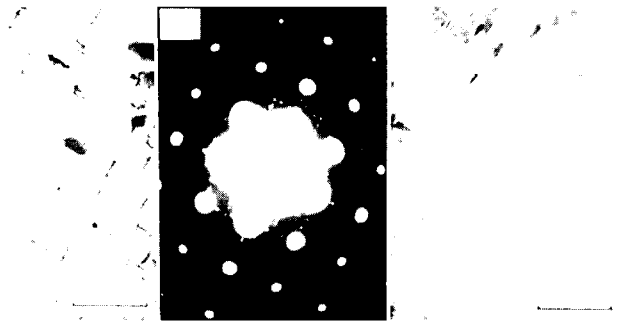

Fig. 3 TEM structures of the LD_{10} alloy aged at 236 ℃ for 24 h
(a)—BFI; (b)—[001]$_\alpha$ zone; (c)—DFI of precipitates

the amount of S phase is not small, at least it is not less than the amount of β or θ phases. It is possible that aging at high temperature (236 ℃) is favorable for the formation of S phase. The DF image formed using the diffraction spots colsed to 110$_\alpha$ is shown in Fig. 3(c). Actually, this image includs S, β and θ' phases because there is no small enough size diaphragm in H-800 microscope to loop a single diffraction spot to form a single precipitate image.

5 CONCLUSIONS

(1) When LD_{10} alloy aged at 236 ℃ for 24 h there are β, θ and S precipition sequences in the LD_{10} alloy. In this condition, the precipitation of S phase is also a primary precipitation sequence.

(2) It is practicable to transform the reciprocal vectors of reflection plane of the precipitates into unit normals vector in the matrix lattice and then to determine their diffraction spot locations on the matrix pattern.

REFERENCES

1 Wang Zhutang *et al*. Handbook of aluminium alloy: physical metallurgy and processing. Changsha: CSUT Press, 1989: 43—56, 240—243.
2 Mondolfo L F. Aluminium Alloy: Structure and Properties, ASM, 1976: 260 — 263, 497 — 503, 566—572.
3 Hatch J E. Aluminium: Properties and Physical Metallurgy, ASM, 1984: 324—337.
4 Chen Yexin *et al* (trans). A crystallography introduction of martensite transformation, Changsha: CSUT Press, 1989: 9—17.
5 Wilson R N *et al*. Acta Metall, 1965, 13: 321.